Monogalactosyldiacylglycerol Deficiency in Arabidopsis Affects Pigment Composition in the Prolamellar Body and Impairs Thylakoid Membrane Energization and Photoprotection in Leaves[1][W][OA]

Henrik Aronsson*, Mark A. Schöttler[2], Amélie A. Kelly[2,3], Christer Sundqvist, Peter Dörmann[4], Sazzad Karim[5], and Paul Jarvis

Department of Plant and Environmental Sciences, University of Gothenburg, SE–405 30 Gothenburg, Sweden (H.A., C.S., S.K.); Max-Planck-Institute of Molecular Plant Physiology, 14476 Golm, Germany (M.A.S., P.D.); Department of Biochemistry and Biophysics, Arrhenius Laboratories for Natural Sciences, Stockholm University, SE–106 91 Stockholm, Sweden (A.A.K.); and Department of Biology, University of Leicester, Leicester LE1 7RH, United Kingdom (P.J.)

Monogalactosyldiacylglycerol (MGDG) is the major lipid constituent of chloroplast membranes and has been proposed to act directly in several important plastidic processes, particularly during photosynthesis. In this study, the effect of MGDG deficiency, as observed in the *monogalactosyldiacylglycerol synthase1-1* (*mgd1-1*) mutant, on chloroplast protein targeting, phototransformation of pigments, and photosynthetic light reactions was analyzed. The targeting of plastid proteins into or across the envelope, or into the thylakoid membrane, was not different from wild-type in the *mgd1* mutant, suggesting that the residual amount of MGDG in *mgd1* was sufficient to maintain functional targeting mechanisms. In dark-grown plants, the ratio of bound protochlorophyllide (Pchlide, F656) to free Pchlide (F631) was increased in *mgd1* compared to the wild type. Increased levels of the photoconvertible pigment-protein complex (F656), which is photoprotective and suppresses photooxidative damage caused by an excess of free Pchlide, may be an adaptive response to the *mgd1* mutation. Leaves of *mgd1* suffered from a massively impaired capacity for thermal dissipation of excess light due to an inefficient operation of the xanthophyll cycle; the mutant contained less zeaxanthin and more violaxanthin than wild type after 60 min of high-light exposure and suffered from increased photosystem II photoinhibition. This is attributable to an increased conductivity of the thylakoid membrane at high light intensities, so that the proton motive force is reduced and the thylakoid lumen is less acidic than in wild type. Thus, the pH-dependent activation of the violaxanthin de-epoxidase and of the PsbS protein is impaired.

Galactolipids are the most abundant nonproteinaceous constituents of plastid membranes. Two galactolipids, monogalactosyldiacylglycerol (MGDG) and digalactosyldiacylglycerol (DGDG), are abundant in plant plastid membranes, where they account for as much as approximately 50 and approximately 20 mol%, respectively, of total lipids (Douce and Joyard, 1990). Because of the different sizes of their head groups, MGDG and DGDG differ in shape and biophysical properties. DGDG has a cylindrical shape that is typical for most plastid lipids and is considered a bilayer-prone lipid. In contrast, MGDG has a conical shape due to its smaller head group and high content of unsaturated fatty acids, giving it nonbilayer-forming characteristics (Webb and Green, 1991; Bruce, 1998).

The synthesis of MGDG predominantly takes place in the inner envelope of chloroplasts (Block et al., 1983; Miège et al., 1999). The enzyme MGDG synthase 1 (MGD1) catalyzes the transfer of Gal from UDP-Gal to *sn*-1,2-diacylglycerol, thus producing MGDG (Benning and Ohta, 2005). The *MGD1* gene, as well as the genes for two other MGDG synthases, *MGD2* and *MGD3*, have been identified in Arabidopsis (*Arabidopsis thaliana*; Miège et al., 1999; Awai et al., 2001). *MGD1*

[1] This work was supported by the Swedish Research Council FORMAS (to H.A.) and VR (to C.S.), by the Wenner-Gren Foundation (to H.A. and A.A.K.), by the Royal Society of Arts and Sciences in Göteborg (to H.A.), by the Royal Swedish Academy of Sciences (to H.A.), by the Deutsche Forschungsgemeinschaft (grant no. SFB429, A12 to M.A.S.; and grant no. SFB429, B6 to P.D.), by the Royal Society Rosenheim Research Fellowship (to P.J.), and by the Biotechnology and Biological Sciences Research Council (to P.J.).

[2] These authors contributed equally to the article.

[3] Present address: HRI/University of Warwick, Wellesbourne, Warwick CV35 9EF, United Kingdom.

[4] Present address: University of Bonn, Institute of Molecular Physiology and Biotechnology of Plants, Karlrobert-Kreiten-Strasse 13, 53115 Bonn, Germany.

[5] Present address: Institute of Biology, University of Tromsø, NO–9037 Tromsø, Norway.

* Corresponding author; e-mail henrik.aronsson@dpes.gu.se.

The author responsible for distribution of materials integral to the findings presented in this article in accordance with the policy described in the Instructions for Authors (www.plantphysiol.org) is: Henrik Aronsson (henrik.aronsson@dpes.gu.se).

[W] The online version of this article contains Web-only data.

[OA] Open Access articles can be viewed online without a subscription.

www.plantphysiol.org/cgi/doi/10.1104/pp.108.123372

is expressed ubiquitously, whereas *MGD2* and *MGD3* are expressed preferentially in flowers and roots (Awai et al., 2001). Expression is uniformly high for *MGD1* during all developmental stages, whereas expression levels of *MGD2* and *MGD3* are much lower (Awai et al., 2001).

We previously identified an MGDG-deficient mutant (*mgd1-1*) that carries a T-DNA insertion in the promoter region of *MGD1* (Jarvis et al., 2000). The T-DNA insertion causes a 75% reduction in *MGD1* mRNA expression, which correlates with a similar reduction in MGDG synthase activity in the mutant. Concentrations of MGDG in mutant leaves are reduced by 42% relative to the wild type. The *mgd1* mutant is less green than the wild type, containing only approximately 50% of the normal amount of chlorophyll (Chl) and displays disturbed plastid ultrastructure. These data led to the conclusion that *MGD1* is responsible for the synthesis of most MGDG in Arabidopsis. Thus, *mgd1-1* is highly suitable for studies on processes in which MGDG is proposed to play an active role, such as chloroplast protein targeting, pigment-protein complex synthesis, and xanthophyll cycle activity.

Chloroplast protein import studies using the Arabidopsis *dgd1* mutant, which is approximately 90% deficient in DGDG, revealed a significant decrease in import efficiency (Chen and Li, 1998). Furthermore, a large number of in vitro studies suggested that MGDG plays an important role during chloroplast protein import (Endo et al., 1992; van't Hof et al., 1993; Pinnaduwage and Bruce, 1996). However, some more recent studies were not consistent with this hypothesis (Inoue et al., 2001; Schleiff et al., 2003). So far, in vivo protein transport studies using an MGDG-deficient mutant have not been reported.

The prolamellar bodies (PLBs) of etioplasts have a high lipid to protein ratio compared to thylakoids. While MGDG is the dominant lipid, NADPH:protochlorophyllide (Pchlide) oxidoreductase (POR) is the most abundant protein in PLBs (Selstam and Sandelius, 1984). An interaction between POR and MGDG has been proposed to stabilize the formation of PLBs (Klement et al., 1999; Engdahl et al., 2001; Selstam et al., 2002). Furthermore, POR is thought to suppress the photooxidative damage caused by inactive or "free" Pchlide acting as a photosensitizer (Runge et al., 1996; Erdei et al., 2005), which is especially important during de-etiolation (Franck et al., 1995). Indeed, overexpression of POR in Arabidopsis plants considerably reduced photooxidative damage (Sperling et al., 1997). Because PLBs can still be observed in *mgd1-1* plants (Jarvis et al., 2000), it is of interest to determine the effect of the MGDG deficiency on the POR-Pchlide-NADPH complex composition in etioplasts.

Several photosynthesis-related reactions are thought to be dependent on galactolipids. For example, the Arabidopsis *dgd1* mutation, which causes DGDG deficiency, affects the composition of the water-oxidizing complex (Reifarth et al., 1997), both photosystems (Dörmann et al., 1995; Härtel et al., 1997), and the levels of xanthophyll cycle pigments (Härtel et al., 1998). The xanthophyll cycle pigment violaxanthin is de-epoxidized into antheraxanthin (A) and then into zeaxanthin (Z) by the enzyme violaxanthin de-epoxidase (VDE). The two latter pigments are believed to facilitate dissipation of excess light energy in the PSII antenna bed during short-term, high-light stress, a process called nonphotochemical quenching (qN; Gilmore and Yamamoto, 1993; Horton et al., 2008). MGDG is the lipid that is most efficient at promoting VDE activity (Yamamoto, 2006); in vitro studies with purified, heterologously expressed VDE have shown that its activity strongly increases in the presence of MGDG (Latowski et al., 2004). In *dgd1*, the de-epoxidation kinetics were accelerated relative to wild type, which was explained by a slight increase in MGDG levels in *dgd1* (Härtel et al., 1998). However, no data on xanthophyll cycle activity in an MGDG-deficient mutant have been presented to date.

The aim of this study was to investigate the in vivo roles of MGDG in various processes in which it is putatively involved, as discussed above. The recently characterized *mgd1* null mutant (*mgd1-2*) has extremely severe defects in chloroplast and plant development (Kobayashi et al., 2007), precluding its use in measurements of chloroplast functions such as those described here. For this reason, we have utilized the original *mgd1-1* mutant, which possesses a leaky or knockdown allele and accumulates approximately 40% less MGDG than wild-type plants (Jarvis et al., 2000).

RESULTS AND DISCUSSION

Protein Targeting Into and Across Chloroplast Membranes Is Not Affected in the *mgd1* Mutant

Based on in vitro studies, MGDG has been suggested to play an important role in protein import into chloroplasts and in the insertion of chloroplast outer envelope membrane proteins (van't Hof et al., 1991, 1993; Chupin et al., 1994; Pilon et al., 1995; Pinnaduwage and Bruce, 1996; Bruce, 1998; Schleiff et al., 2001; Hofmann and Theg, 2005). While previous analyses using the Arabidopsis *dgd1* mutant clearly demonstrated the importance of DGDG for efficient chloroplast protein import (Chen and Li, 1998; Aronsson and Jarvis, 2002), the role of MGDG in protein targeting processes has not previously been tested in vivo. To address this issue, import studies with *mgd1* chloroplasts were done using three nucleus-encoded precursor proteins: the small subunit of Rubisco (pSS; a photosynthetic preprotein), the 50S ribosomal subunit protein L11 (pL11; a nonphotosynthetic preprotein), and subunit II of CF_0 of the photosynthetic ATPase (pCF_0II; a preprotein that engages the spontaneous thylakoid targeting pathway after chloroplast import; Fig. 1A). Import efficiency was measured using time course experiments. The appearance of the smaller,

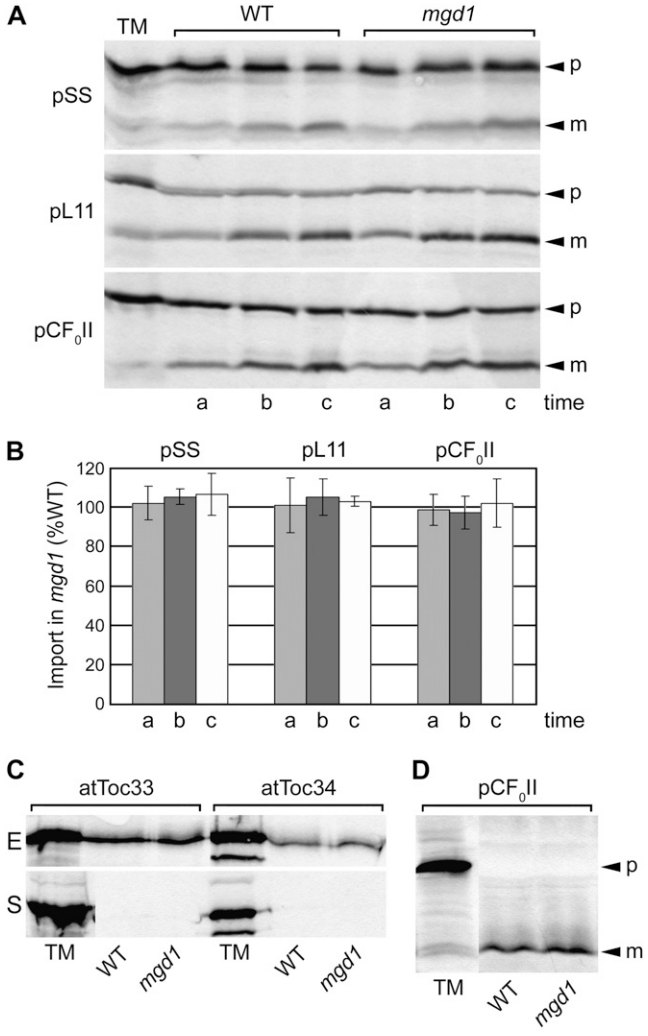

Figure 1. Chloroplast protein translocation and insertion assays. A, Import of different precursor proteins into wild-type and *mgd1* mutant Arabidopsis chloroplasts. Import reaction time points are defined as follows: a, 3 min (1 min for pL11); b, 6 min (2 min for pL11); c, 10 min (3 min for pL11). Note that for pL11, a shorter time series was used (1–3 min instead of 3–10 min for the other precursors) because pL11 is known to have a faster import rate (Aronsson and Jarvis, 2002). TM, Translation mixture; p, precursor protein; m, mature protein. B, Quantification of the import data shown in A. The amount of imported, mature protein in *mgd1* chloroplasts is expressed as percentage of the amount of imported protein in wild-type chloroplasts (set to 100%). Values shown are means (±SD) derived from at least three assays. C, Direct insertion into the outer envelope membrane. In vitro-translated atToc33 and atToc34 proteins were incubated with wild-type and *mgd1* chloroplasts for 30 min under import conditions and then subjected to treatment with Na_2CO_3, pH 11.5. The treated samples were then divided into a soluble (S) and an envelope-enriched (E) fraction prior to analysis. D, Direct insertion into the thylakoid membrane by the spontaneous pathway. In vitro-translated pCF_0II was incubated with wild-type and mutant chloroplasts under import conditions for 30 min. At the end of the import reaction, thermolysin treatment was used to remove any unimported preprotein, and then thylakoid membranes were isolated.

mature form of each protein, due to transit peptide cleavage, was taken to indicate that import had occurred (Fig. 1A). All three proteins were imported and, in all cases, import was time dependent. Surprisingly, protein import efficiency in *mgd1* chloroplasts was similar to that in wild-type chloroplasts; none of the proteins tested showed any significant difference in import efficiency between wild-type and mutant chloroplasts (Fig. 1B).

Next, we assessed the possibility that protein insertion into the outer envelope membrane is affected by *mgd1* because MGDG has been suggested to facilitate protein recognition during such targeting processes (Pinnaduwage and Bruce, 1996). We used two different outer envelope membrane proteins, atToc33 and atToc34, both of which lack a transit peptide (like most outer envelope proteins; Hofmann and Theg, 2005). However, we again observed no defect in protein targeting efficiency in the *mgd1* mutant. Both proteins inserted equally well into the outer envelope membrane of wild-type and mutant chloroplasts (data not shown), and the inserted proteins withstood extraction by alkaline treatment to the same extent (Fig. 1C, top) such that no protein was extracted to the soluble supernatant fraction (Fig. 1C, bottom), clearly demonstrating that insertion efficiency was not affected by the *mgd1* mutation. These results are similar to those reported previously for OEP14 for the *dgd1* mutant (Chen and Li, 1998), suggesting that galactolipids may not play an important role in the insertion of outer envelope proteins in vivo. However, OEP14 is a signal-anchored protein, whereas atToc33 and atToc34 are tail-anchored proteins, and it is presently not clear if these different protein classes use the same or different insertion mechanisms (Hofmann and Theg, 2005).

Because MGDG is the major lipid constituent of thylakoid membranes and because CF_0II targeting follows the spontaneous thylakoid insertion pathway that does not appear to depend on any proteinaceous factors (Michl et al., 1994; Jarvis and Robinson, 2004), we went on to conduct pCF_0II thylakoid insertion experiments. Following chloroplast import reactions, plastids were treated with thermolysin to avoid possible contamination from envelope-bound CF_0II, and then thylakoids were isolated and analyzed (Fig. 1D). However, the results revealed that the spontaneous insertion pathway was not significantly affected by the *mgd1* mutation because equal amounts of protein were inserted into wild-type and mutant thylakoids. Thus, either the level of galactolipids in *mgd1* is sufficient to retain a competent spontaneous insertion pathway, or, alternatively, the role of lipids (and of MGDG specifically) in this pathway is not significant.

Immunoblots were prepared to study the levels of proteins involved in the chloroplast import mechanism (atToc33 and atToc75-III), as well as of some substrates of the import machinery (atToc75-III, Lhcb2, PsaD, PsbS, plastocyanin [PC], and VDE; note that D1, PsbB, PsaC, and β-ATPase are encoded by the plastome and so do not need to be imported), in wild-type and *mgd1* plants (Fig. 2). The chloroplast import machinery consists of several different components; the atToc33 and atToc75-III proteins tested here contribute

to the receptor and channel-forming functions, respectively, in the outer envelope membrane (Bédard and Jarvis, 2005). For protein import to proceed efficiently, as was seen for pSS, pL11, and pCF_0II (Fig. 1, A and B), one would expect the expression of translocon components like these to remain largely unchanged. As shown in Figure 2, both atToc33 and atToc75-III are expressed in wild-type and *mgd1* plants at similar levels. Similarly, all proteins tested that must be imported into the chloroplast through the TOC/TIC machinery were also present at normal levels in the *mgd1* mutant (Fig. 2).

Thus, our data suggest that MGDG may not be as important for chloroplast protein targeting as was suggested on the basis of earlier, in vitro studies. The many proteins normally present in chloroplast membranes are missing in the artificial membrane systems used for such in vitro experiments, and so the MGDG dependency observed in those studies may have been an overestimation. Alternatively, our negative results may be related to the fact that *mgd1-1* contains only 42% less MGDG than the wild type, or indicate that some of the other lipids compensate for the loss of MGDG in the mutant (Jarvis et al., 2000). It is conceivable that a larger MGDG reduction would cause significant targeting defects. However, in the extreme case of the *mgd1-2* null mutant (Kobayashi et al., 2007), plant and chloroplast development are so badly affected that analysis and interpretation would both be extremely problematic.

Our results (in particular, Fig. 1, A and B) contrast with those reported previously for the *dgd1* mutant (Chen and Li, 1998; Aronsson and Jarvis, 2002). This may indicate that DGDG is relatively more important for chloroplast import than MGDG. This possibility is supported by the observation that DGDG was the only galactolipid associated with the TOC translocon complex (Schleiff et al., 2003) and by the fact that in *mgd1* the level of DGDG is not altered (Jarvis et al., 2000). An alternative explanation for the different results obtained with *dgd1* is that this mutant has a much more severe lipid defect: the *dgd1* mutant has a 90% reduction in DGDG levels (Dörmann et al., 1995).

Fluorescence Measurements Reveal Increased Pchlide-F656 Levels in Etiolated Plants

An interaction between POR and MGDG has been proposed to stabilize the formation of the etioplast structure in darkness and to increase the fluorescence of Pchlide at around 655 nm (Klement et al., 1999; Engdahl et al., 2001; Selstam et al., 2002). These observations, together with the alterations in plastid structure seen in *mgd1* (Jarvis et al., 2000), led us to investigate the effect of MGDG deficiency on the assembly of plastid internal membranes, either developed in darkness as PLBs and prothylakoids or in the light as thylakoids. The fluorescence from pigment-protein complexes consisting of Pchlide, NADPH, and POR can be used to assess how MGDG deficiency affects the plant's strategy for the use of incoming light and for protection against an excess of light.

The hook of dark-grown seedlings was subjected to rapid freezing in liquid nitrogen (77 K), and then fluorescence emission was recorded after excitation at 440 nm. Measurements of wild-type samples revealed a lower emission peak for Pchlide-F656 than for Pchlide-F631. By contrast, the *mgd1* mutant had a higher peak at 656 nm, significantly increasing the ratio of Pchlide-F656 to Pchlide-F631 relative to the wild type (Fig. 3A). This pattern was even more pronounced when an excitation wavelength of 460 nm was used (data not shown).

Pchlide-F631 is the first form of the pigment to be produced during plastid development, and it is referred to as nonphotoactive Pchlide because it cannot participate in Chl formation (it is in a free or unbound state). By contrast, Pchlide-F656 corresponds to photoactive Pchlide bound to POR. Previous work has suggested that Pchlide-F631 (or an equivalent species) is a photosensitizer, rendering plants susceptible to photooxidative damage (Runge et al., 1996; Sperling et al., 1997; Erdei et al., 2005).

The photoactivity of Pchlide-F656 was verified by flash illumination. The dark-grown 5-d-old seedlings stored at 77 K were rewarmed to 253 K (−20°C), flashed with strong light, and then immediately frozen in liquid nitrogen (77 K); thereafter, the emission spectra were recorded (Fig. 3B). The 2-fold higher levels of the chlorophyllide (Chlide)-F688 fluorescence peak in *mgd1* can be taken as further evidence for the increased amount of photoactive Pchlide-F656 in the mutant (Fig. 3B). Measurements of dark-grown seedlings of different ages (5, 7, and 8 d old) always revealed an increase in the Pchlide-F656 form in the mutant, excluding the possibility that the differences in fluorescence were due to developmental stage differences (data not shown). To further verify the observed increase in formation of Chlide in *mgd1*, the degree of phototransformation was determined. A predetermined fluorescence ratio between Pchlide and Chlide of 1.09 (Ryberg and Sundqvist, 1982) was

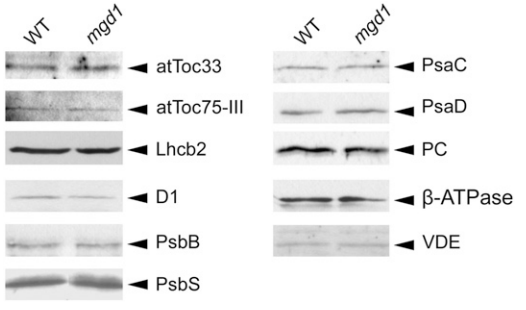

Figure 2. Immunodetection of different chloroplast proteins. Chloroplasts were isolated from 2-week-old wild-type and *mgd1* mutant plants and used to prepare immunoblots. Equal (10 μg or 1 μg for PsbS) samples of total chloroplast protein were loaded per lane, and the blots were used to compare levels of several different proteins, as indicated. Antibodies were detected using an ECL system (Amersham Biosciences).

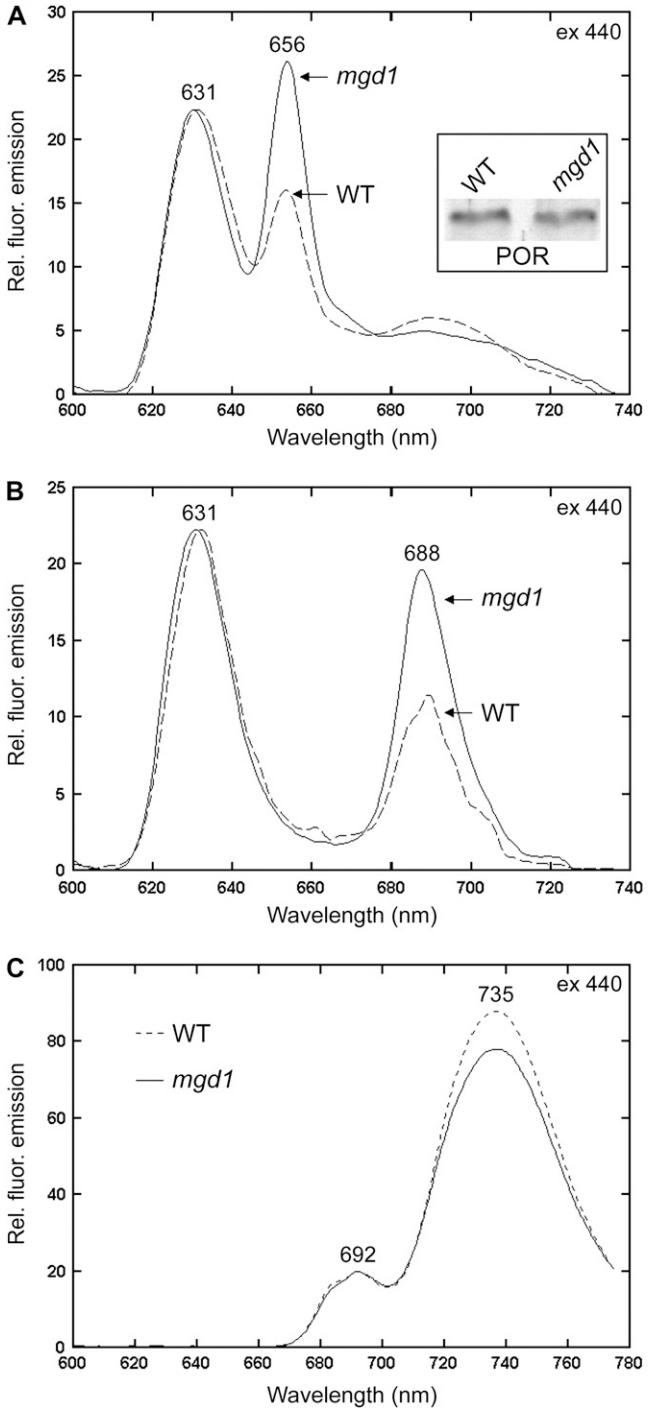

Figure 3. Low-temperature (77 K) fluorescence emission spectra. Fluorescence emission spectra were recorded using the following wild-type and *mgd1* mutant samples: A, the cotyledons of 5-d-old dark-grown plants; B, the cotyledons of 5-d-old flash-irradiated, dark-grown plants; C, the leaves of 28-d-old plants grown at approximately 200 μmol m^{-2} s^{-1}. The spectra were normalized at 631 nm (A and B) or 705 nm (C). Excitation wavelength was 440 nm in each case, as indicated. The inset in A shows an immunoblot performed on total protein samples isolated from 5-d-old dark-grown plants and indicates the level of total POR protein. In B, a flash lamp (Braun F 800 Professional) with the effect of 165 W and a duration of 1 ms of the flash was used for phototransformation.

used to determine the degree of phototransformation of Pchlide to Chlide. The values obtained were always higher for *mgd1*; after one flash, *mgd1* gave 51% and wild type gave 45%; after two flashes, the results were 65% and 49%; and, after three flashes, the results were 74% and 64%. Altogether, the data convincingly show that *mgd1* has a higher yield of phototransformation of Pchlide into Chlide than the wild type. These results are consistent with the increased level of photoactive Pchlide-F656 observed in *mgd1* (Fig. 3A).

Previous work demonstrated that overexpression of POR increases the Pchlide F656 to F631 ratio (equivalent to the F655 to F632 ratio; Franck et al., 2000) and protects the photosynthetic apparatus against photooxidative damage (Sperling et al., 1997). Thus, a low Pchlide F656 to F631 ratio is associated with susceptibility to oxidative damage. Our results suggest that a mechanism to avoid this scenario is activated in the *mgd1* mutant. However, this mechanism does not appear to involve up-regulated expression of POR because steady-state levels of the protein were unaltered (Fig. 3A, inset). The increased Pchlide F656 to F631 ratio in *mgd1* may indicate that Pchlide-F656 formation is favored. This not only would serve to minimize the possibility for photooxidative damage but also would maximize the use of incoming light for Pchlide to Chlide transformation, enabling the proper conversion of PLBs and prothylakoids into thylakoids.

The observed differences in pigment-protein composition in dark-grown *mgd1* plants (Fig. 3, A and B) are interesting because etioplasts in 5-d-old *mgd1* plants were reported to have normal ultrastructure (Jarvis et al., 2000). Therefore, the increase in Pchlide-F656 is due neither to a lack of prothylakoids, which predominantly contain Pchlide-F631, nor to an increase in PLBs, which are highly enriched in Pchlide-F656 (Ryberg and Sundqvist, 1982). This is in agreement with our hypothesis that the accumulation of photoactive Pchlide-F656 (at the expense of nonphotoactive Pchlide-F631) is not simply a passive response but, rather, is part of an adaptive mechanism designed to protect the photosynthetic apparatus against excess light. This may be related to the fact that another photoprotective mechanism (the xanthophyll cycle) is compromised in the *mgd1* mutant (see below).

We also investigated the role of MGDG in determining the composition of pigment-protein complexes in thylakoids of light-grown plants (Fig. 3C). No obvious differences in the fluorescence emission for PSII and PSI were observed in plants grown at low light intensity (approximately 100 μmol m^{-2} s^{-1}; data not shown). However, when plants were grown at an elevated light intensity of approximately 200 μmol m^{-2} s^{-1}, the fluorescence at around 735 nm was decreased in *mgd1* (Fig. 3C). The relative fluorescence intensity at 692 nm, which reflects PSII, was similar for *mgd1* and wild type at the light intensity used (Fig. 3C). Because the ratio of the peaks at 692 and 735 nm is a measure for the antenna cross sections of the two photosystems relative to each other, these data suggest

that either the accumulation of PSI reaction centers relative to PSII is reduced or that the distribution of light-harvesting complex (LHC) proteins between PSI and PSII is altered in *mgd1* at elevated light intensities.

MGDG Is Required for Efficient Photosynthesis and Photoprotection of Thylakoids

Chloroplast ultrastructure was previously reported to be altered in *mgd1* (Jarvis et al., 2000). Not only is MGDG a major constituent of the lipid matrix of the photosynthetic membranes, but, as revealed by crystallization studies, it is also an integral component of PSI, PSII, and the cytochrome b_6f complex (Jordan et al., 2001; Stroebel et al., 2003; Loll et al., 2005). Thus, the MGDG-deficiency of *mgd1* might be expected to cause alterations in photosynthetic performance.

To assess this possibility, we first measured photosynthetic pigment composition in light-adapted plants. Pigments levels were analyzed by HPLC and are presented as nanomoles per gram fresh weight in Table I. The total amount of pigments is reduced by approximately 29% in *mgd1* relative to wild type due to a 30% reduction in total Chl and a 23% reduction in carotenoids. In *mgd1*, Chl *a* is reduced by approximately 28%, and an even stronger reduction is observed for Chl *b* (35%); these changes are reflected in an increased Chl *a* to *b* ratio in the mutant (3.3 in wild type; 3.6 in *mgd1*). The increased Chl *a* to *b* ratio suggests a preferred maintenance of Chl *a*-rich reaction centers at the expense of Chl *b*-rich antenna complexes (which may be a mechanism to enable more efficient use of light energy with limited pigment resources). The quantification of photosynthetic complexes and low-temperature Chl *a* fluorescence measurements is certainly supportive of this interpretation (see below).

The major carotenoid pigment, lutein, was reduced in abundance in *mgd1* by 33.7% (on a per fresh weight basis; Table I). Moreover, the amounts of all xanthophyll cycle pigments were reduced in *mgd1* (Table I). V was reduced by 8.5%, Z was reduced by 37.5%, and neoxanthin was reduced by 33.7% (all on a per fresh weight basis). When the pigment concentrations were normalized to the amount of Chl *a* (mmol pigment/mol Chl *a*; Table I), most pigment values were still reduced in *mgd1* relative to wild type.

To characterize the function of the electron transport chain, the quantum yield of PSII, a measure of photosynthetic efficiency, was determined in dark-adapted leaves (F_v/F_m). Measurements of F_v/F_m in wild type and *mgd1* were indistinguishable (data not shown), indicating that a reduction in MGDG content of approximately 40% has no impact on photosynthetic efficiency in low-light-grown plants. Next, we determined light saturation curves of linear electron transport from PSII yield measurements. Because the absorption properties of wild-type and *mgd1* leaves were unaltered, despite the approximately 30% reduction in pigments, and because quantification of the photosynthetic complexes indicated only a minor change in the stoichiometry of the photosystems and their antenna cross sections (see below), it is legitimate to calculate linear electron flux from PSII quantum efficiency (Genty et al., 1989). These measurements revealed a 30% reduction of linear electron flux capacity per leaf area in the *mgd1* mutant (Fig. 4A). These data are independently supported by gas exchange measurements, revealing an approximately 25% reduction of light- and CO_2-saturated leaf assimilation capacity per leaf area in the mutant (18.7 ± 2.5 μmol CO_2 m^{-2} s^{-1} in the wild type; 13.9 ± 3.7 μmol CO_2 m^{-2} s^{-1} in *mgd1*).

While the diminished linear electron flux and assimilation rate per leaf area point to a reduced efficiency of photosynthesis in *mgd1* (Fig. 4A), the functional organization of the electron transport chain does not seem to be strongly affected by MGDG deficiency in *mgd1*; when electron transport rates are recalculated on a Chl basis (e.g. per photosynthetic unit), they were comparably high in *mgd1* and the wild type. This was confirmed by quantifications of the photosynthetic com-

Table I. *Pigment composition in wild-type and mgd1 mutant Arabidopsis plants*

Plants were 35 to 42 d old and were grown under a 16-h-light/8-h-dark cycle with a light intensity of approximately 100 to 150 μmol m^{-2} s^{-1}. Data are mean values (±SE) derived from four independent samples and are expressed as nanomoles per gram fresh weight and as millimoles per mole Chl *a*.

Pigment or Ratio	Wild Type	*mgd1*	Wild Type	*mgd1*
	nmol g^{-1} fresh weight		*mmol mol^{-1} Chl a*	
Neoxanthin	40.44 ± 6.73	26.83 ± 2.80	35.03 ± 2.44	32.78 ± 3.2
V	32.67 ± 5.86	29.90 ± 4.30	28.18 ± 2.7	36.03 ± 3.3[a]
A	1.21 ± 0.18	0.82 ± 0.04[a]	1.08 ± 0.34	1.02 ± 0.17
Z	6.94 ± 1.28	4.34 ± 0.43[a]	5.99 ± 0.74	5.31 ± 0.41
Lutein	127.29 ± 18.21	84.35 ± 9.04[a]	111.09 ± 3.79	102.81 ± 6.08[a]
β-Carotene	33.72 ± 13.33	39.50 ± 14.40	30.74 ± 25.2	45.33 ± 29.37
DES (A + Z)/(V + A + Z)			0.201 ± 0.012[b]	0.151 ± 0.012[a,b]
Chl *a*	1,140.25 ± 145.66	820.66 ± 84.06	1,000 ± 0	1,000 ± 0
Chl *b*	349.10 ± 45.50	227.29 ± 23.83[a]	305.93 ± 2.99	276.97 ± 9.48[a]
Chl *a*/Chl *b*	3.27 ± 0.032[b]	3.61 ± 0.061[a,b]		

[a]Statistically significant differences from control values, as calculated using a Student's *t* test ($P \leq 0.05$). [b]These values are ratios and so do not have units.

plexes by means of immunoblotting (Fig. 2) and difference absorption spectroscopy (Table II).

Components analyzed by immunoblotting were as follows. For PSII, we analyzed the antenna complex polypeptide, Lhcb2, the two essential core complex proteins, D1 and PsbB, and PsbS localized at the periphery of PSII. For PSI, we analyzed PsaC and PsaD, which are localized at the periphery of PSI but which nevertheless represent reasonable indicators of PSI abundance, as in the absence of PsaC, no stable accumulation of PSI is possible (Takahashi et al., 1991). We also analyzed two proteins (PC and the β-subunit of the ATP synthase) not directly associated with either PSII or PSI but that are nonetheless important to maintain optimal photosynthesis. As shown in Figure 2, none of these proteins was expressed at significantly different levels in *mgd1* relative to wild type. The results presented in Figure 1 are also consistent with this conclusion.

These conclusions are supported by difference absorption spectroscopy data (Table II). While the content of PSII was slightly increased in the mutant (approximately 120% of the wild-type level), the contents of the cytochrome b_6f complex, PSI, and PC were similar in the wild type and mutant. The slight elevation of PSII content, which is below the resolution of our immunoblot analysis, may explain the increased Chl *a* to *b* ratio of the mutant; because the PSI content was unaffected, the ratio increase can only be explained by the loss of LHC antenna proteins of the photosystems, as alluded to earlier. This conclusion is in line with 77-K Chl *a* fluorescence emission signals determined on leaves of 28-d-old plants; the PSI fluorescence emission signal at 735-nm wavelength is slightly smaller in the wild type than in the mutant, which is in agreement with a slightly elevated PSII to PSI ratio in *mgd1* thylakoids (Fig. 3C).

qN Is Impaired in the *mgd1* Mutant

In addition to having lower photosynthesis capacity per unit leaf area (Fig. 4A), Chl *a* fluorescence light response curves revealed that *mgd1* has a much lower capacity for qN (qN is approximately 0.8 and 0.55 in wild-type and *mgd1* leaves, respectively, at light intensities exceeding 1,000 μmol m^{-2} s^{-1}; Fig. 4B). Consequently, the *mgd1* mutant was clearly more susceptible to light stress. After leaves had been exposed to 1,000 μmol m^{-2} s^{-1} of actinic light for 1 h, the proportion of photoinhibited PSII was calculated from the dark-relaxation kinetics of qN. The qI component, the fraction of qN relaxing with a half-time >15 min (which correlates with PSII photoinhibition; Krause and Weis, 1991), was much larger in mutant than in wild-type leaves (0.25 versus 0.11, respectively), confirming that PSII in *mgd1* is much more prone to photoinhibition under light-stress conditions. Thus, the reduction in the rapidly reversible component of qN (qE), which is related to thermal dissipation of excess energy in the PSII antenna bed, can be concluded to be even more dramatically impaired in *mgd1* than suggested by their lower qN values in saturating light.

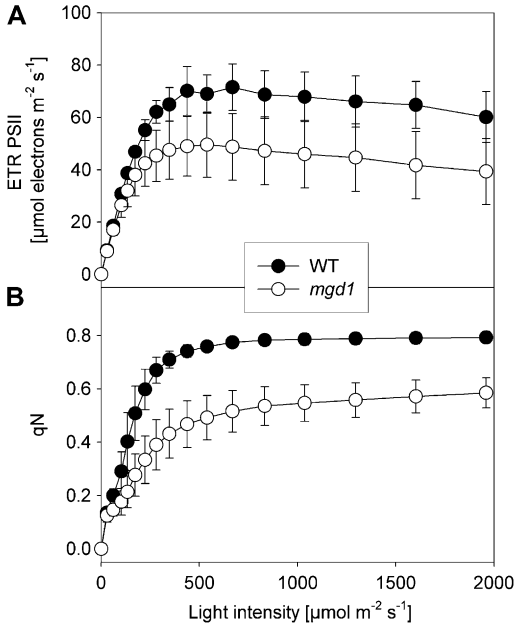

Figure 4. Light response curves for linear electron transport and qN. A, Linear electron transport was calculated from PSII quantum yield in wild-type and *mgd1* mutant plants according to Genty et al. (1989). Five-week-old plants grown in normal light (150 μmol m^{-2} s^{-1}) were measured without further treatment. Data shown are means (±SD) derived from measurements of five different plants per genotype. Black symbols, wild type; white symbols, *mgd1*. B, qN was calculated using the data shown in A according to Krause and Weis (1991).

Reductions in the capacity of qN could be due to any of several possible defects in the *mgd1* mutant because qE is essentially induced by acidification of the thylakoid lumen (which is itself influenced by numerous factors). Under standard growth conditions used during this study, the pH of the thylakoid lumen is predicted to be in the region of 6.5 (Takizawa et al., 2007). Upon high-light stress, it decreases and triggers photoprotective mechanisms via changes in the PSII antenna system. The PsbS protein, which is involved in thermal dissipation, is protonated and initiates a conformational change in the PSII-LHCII supercom-

Table II. *Amounts of the photosynthetic complexes and of PC as determined by difference absorption spectroscopy*

Data are mean values (±SE) derived from five independent thylakoid isolations and are expressed as millimoles of each component per mole Chl.

Complex or Component	Wild Type	*mgd1*
	mmol mol Chl^{-1}	
PSII	2.38 ± 0.16	2.86 ± 0.13
Cytochrome b_6f complex	1.06 ± 0.10	1.04 ± 0.08
PC	9.27 ± 0.78	9.52 ± 0.86
PSI	2.22 ± 0.41	2.28 ± 0.28

plexes. This change in the PSII antenna bed is further stabilized by the de-epoxidation of V to Z by the luminal VDE (Horton et al., 2008). VDE is only activated when the pH of the thylakoid lumen falls below 6.8 (Takizawa et al., 2007). Hence, reductions in the capacity of qN could be due to reductions in the amounts of PsbS or VDE, or impairment of the function of VDE because all of these chloroplast components affect qE. It has been shown that MGDG is the major lipid that is directly associated with VDE activity (Yamamoto, 2006) and that VDE is dependent on MGDG for optimum activity in vitro (Latowski et al., 2004). Furthermore, any alteration in the thylakoid membrane's proton conductivity could directly affect qE, if the threshold acidification required for the activation of PsbS and VDE is not reached.

VDE and PsbS Activities Remain Unchanged and Do Not Contribute to Changes of the Xanthophyll Cycle

To assess the different factors possibly contributing to alterations in qN and qE in *mgd1*, we first checked for changes in the levels of PsbS and VDE by immunoblotting. However, we detected no change in the abundance of either protein in the mutant (Fig. 2). Next, to compare in vivo parameters of the xanthophyll cycle in the mutant and wild type, we measured the kinetics of V de-epoxidation in leaves of plants that had first been adapted to complete darkness for 2 h and which were then exposed to strong light (approximately 1,000 μmol m^{-2} s^{-1}) for up to 60 min. The measured amounts of V, A, and Z were normalized to the total pool size of xanthophyll cycle pigments and then plotted against the duration of exposure to high light (Fig. 5). Following dark adaptation, wild-type and mutant plants both contained high amounts of V, very low amounts of A, and no detectable Z (see 0-min data points; Fig. 5, A and B), due to the inactivation of VDE in darkness. Immediately after the onset of light, the level of V rapidly declined in both genotypes, while the levels of A and Z both increased (Z to a much higher value than A).

In wild-type leaves, the molar proportion of V initially dropped in the first 10 min to less than 40% and then remained constant throughout the remainder of the experiment (Fig. 5A). The proportion of V in *mgd1* leaves also declined to approximately 40%, during the first 5 min, but in contrast to wild-type leaves, it progressively increased thereafter, reaching 55% after 60 min (Fig. 5B). For both genotypes, the molar proportion of A increased from 5% to approximately 20% to 25% during the first 10 min but then slightly decreased to approximately 15% to 20% after 60 min (Fig. 5, A and B). The changes in molar proportions of Z appeared to be directly opposite to, and were presumably due to, alterations in the abundance of V; levels of Z initially increased rapidly in both wild-type and *mgd1* leaves but then remained at a higher level (approximately 45%–50%) in wild-type leaves, while they declined in *mgd1* leaves before reaching a plateau during the latter part of the experiment (Fig. 5B). Thus, prolonged illumination with high light over a period of 60 min had a severe impact on the ratio of V to Z in *mgd1* plants. These changes were reflected in differences in de-epoxidation status (DES; =[A + Z]/[V + A + Z]) between wild-type and mutant plants (Fig. 5C).

The reduced steady-state capacity of the xanthophyll cycle in *mgd1* could be due to either impaired enzyme activity or reductions in the proton motive force (*pmf*) across the thylakoid membrane. However, the former possibility seems to be highly unlikely because reductions in enzyme activity should have affected both the rapid generation of A and Z during the first 5 min of light stress (Fig. 5) and the steady-state DES. Because no delay in V de-epoxidation was observed in *mgd1* plants, a general impairment of VDE activity is unlikely to be the cause of the reduction in Z levels during the latter period of the light stress experiment (Fig. 5). Nevertheless, we examined VDE enzyme activities in wild-type and *mgd1* samples in vitro under pH-induced dark conditions. However, as expected, no significant differences in VDE enzyme activities were detected between the wild-type and mutant samples (Supplemental Fig. S1). Because the lower qE and reduced levels of Z under light-stress conditions could not be explained by changes in PsbS or VDE protein levels, or by alterations in VDE activity, we next assessed the possibility that *mgd1* causes alterations in the steady-state *pmf* across the thylakoid membranes.

Reduced Electrochromic Signal Amplitudes in *mgd1* Confirm Impaired *pmf* Formation Across the Thylakoid Membrane

To obtain information on the thylakoidal *pmf*, we measured electrochromic signals (ECS); these are carotenoid absorption shifts with kinetic properties that are proportional to the relative contributions of the electric ($\Delta\Psi$) and osmotic (ΔpH) components of the *pmf* and overall amplitudes that are proportional to the total *pmf* (Kramer et al., 2003; Cruz et al., 2005; Takizawa et al., 2007). The maximum *pmf*, determined from the dark-interval relaxation of the ECS after illumination with saturating light, was more than 60% lower in *mgd1* leaves than in wild-type leaves (data not shown). Even after normalizing the signal to the Chl contents, a dramatic reduction (>40%) in the maximum *pmf* relative to wild type was observed (Fig. 6A; see data points at 2,100 μmol m^{-2} s^{-1} actinic light intensity). To ensure that the observed reduction in the ECS amplitude in *mgd1* did not result from changes in the optical properties of the leaves, we also measured cytochrome *f* reduction kinetics during the dark interval (data not shown). Any artefacts resulting from changes in the optical properties of the leaves should have had similar effects on the two signals because they are measured in the same wavelength range. However, after normalization of the cytochrome *f*

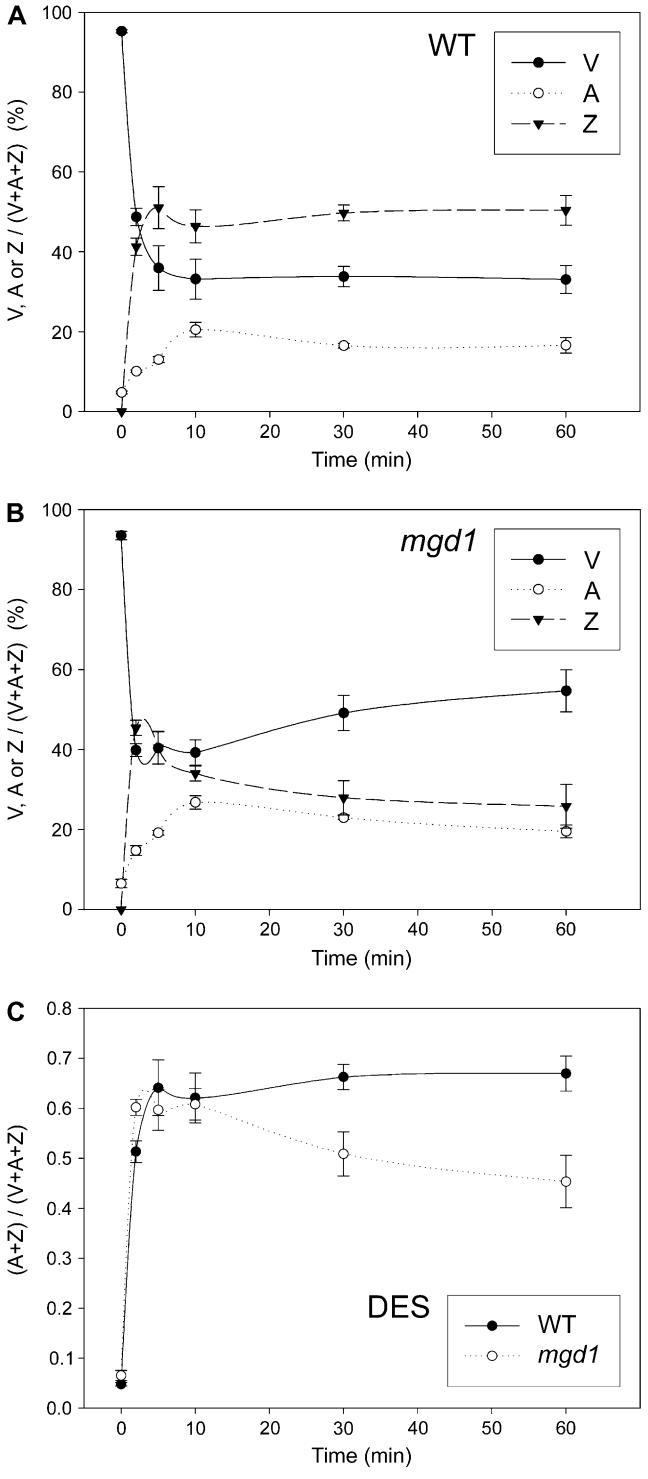

Figure 5. Xanthophyll cycle measurements. Dark-adapted plants (0 min) were moved to a high-light chamber (1,000–1,100 μmol m^{-2} s^{-1}), and xanthophyll cycle pigments were measured by HPLC at the indicated time points. The relative concentrations of V, A, and Z in wild-type (A) and *mgd1* mutant (B) plants are shown. Values for each pigment are expressed as a percentage of the total xanthophyll pool in each sample. Data shown are means (±SD) derived from at least five measurements. C, The DES of the wild-type and mutant plants was calculated for each time point, using the data shown in A and B. Values were calculated as follows: DES = (A + Z)/(V + A + Z).

difference absorption signals to leaf Chl contents, there were no significant differences; this is in accordance with the quantification of the cytochrome b_6f complex in isolated thylakoids, which was also found to be unaltered in *mgd1* (Table II). Therefore, the observed difference in the ECS amplitude clearly indicates that there is an approximately 40% reduction in *pmf* across the thylakoid membrane in *mgd1*, confirming that the mutant's capacity for thylakoid membrane energization is strongly reduced.

Reduced qN Capacity in *mgd1* Is Due to Increased Conductivity of the Thylakoid Membranes

Next, we examined the relationship between *pmf* and actinic light intensity in wild-type and mutant leaves (Fig. 6A). The results showed that the *pmf* of the mutant leaves was almost as high as in wild-type leaves under light-limited conditions (200 μmol m^{-2} s^{-1} light). However, at higher light intensities, when qN becomes more important as a photoprotective mechanism, the increase in *pmf* was much weaker in *mgd1* than in the wild type, resulting in the approximately 40% reduction in maximum *pmf*.

The reduced *pmf* under high light intensities indicates that the thylakoid lumen might be considerably less acidic in *mgd1* than in wild type, impeding full activation of the VDE and PsbS proteins. This hypothesis could explain the mutant's reduced qN capacity. However, the induction of qN is not dependent on total *pmf* but only on the ΔpH component (Cruz et al., 2005; Takizawa et al., 2007). Because the partitioning of *pmf* into ΔpH and $\Delta\Psi$ is highly variable between species and individuals (Takizawa et al., 2007) and the amplitude of the ECS reflects both the $\Delta\Psi$ and ΔpH components of the *pmf*, we next had to discriminate between the contributions of the two components. This was done by measuring the slow phase (in the range of seconds) of ECS relaxation in darkness, which is attributable to counter-ion movement across the thylakoid membrane (Takizawa et al., 2007). Surprisingly, we found approximately 50:50 partitioning of the *pmf* between the ΔpH and $\Delta\Psi$ components, regardless of the actinic light intensity, in both wild-type and *mgd1* mutant leaves (Fig. 6B). Therefore, the reduced total *pmf* amplitude observed in *mgd1* must correlate with a similar (>40%) reduction in maximum thylakoid lumen acidification. As described below, this would keep the thylakoid lumen pH above the threshold level required for full activation of PsbS and VDE.

The lumenal pH at maximum acidification is believed to be approximately 5.7 (Takizawa et al., 2007); below this pH, photosynthesis is strongly inhibited due to the loss of electron transfer activities of the cytochrome b_6f complex, PSII, and PC (Krieger and Weis, 1993; Kramer et al., 1999). The pH of the thylakoid lumen in dark-adapted leaves is believed to be approximately 7.5, i.e. only slightly lower than the stromal pH (Takizawa et al., 2007). Considering these

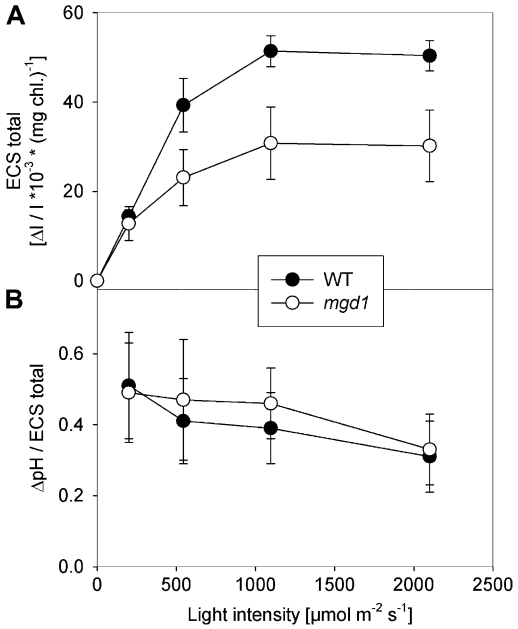

Figure 6. Thylakoid membrane energization is strongly reduced in the *mgd1* mutant at high light intensities. A, Light response curve of the total ECS, which is proportional to the steady-state *pmf* across the thylakoid membrane. The *pmf* across the thylakoid membrane during steady-state photosynthesis was estimated from the amplitude of the ECS during short intervals (15 s) of dark relaxation. Leaves of 5-week-old plants grown in normal light (150 μmol m^{-2} s^{-1}) were preilluminated at each light intensity for 10 min to allow photosynthesis to reach steady state, and the total ECS was normalized to the Chl content of the leaf segment being measured. B, Contribution of the ΔpH to the total *pmf* across the thylakoid membrane. Estimates of the partitioning of *pmf* between its ΔpH and $\Delta\Psi$ components were derived from measurements obtained during the slowly relaxing phase of the ECS. Data shown in A and B are means (±SD) of measurements of six different plants per genotype. Black symbols, wild type; white symbols, *mgd1*.

two values and the fact that the maximum total *pmf* and the ΔpH component are both reduced by approximately 40% to 50% in *mgd1* plants, one can estimate that the lumenal pH in the mutant is in the region of 6.5. Because PsbS and VDE just begin to be activated when the lumen pH falls to around this value and full qE is only established when the pH falls below 6.0 (Takizawa et al., 2007), one can deduce that the reduced qN capacity of *mgd1* is entirely explainable in terms of increased conductivity of the thylakoid membranes in saturating light.

Alteration of the steady-state energization of the thylakoid membrane may also explain the declines in Z content and DES observed in *mgd1* after 5 min of high-light stress (Fig. 5). Immediately after illumination of dark-adapted leaves, the *pmf* is dramatically higher than under steady-state conditions because both the Calvin cycle (which consumes ATP) and the ATP synthase are still inactive, and their reductive activation by thioredoxin takes a few minutes in the light; a lower steady-state *pmf* is established only after ATP synthase activation because part of the *pmf* is then used for ATP synthesis. Therefore, in both wild-type and *mgd1* mutant leaves, *pmf* is highest during the activation phase of photosynthesis and then subsequently declines to steady-state levels within 10 min following the onset of illumination. Hence, the *pmf* in the *mgd1* mutant is only high enough to fully activate VDE during the first few minutes of illumination; later, under steady-state conditions, the *pmf* in *mgd1* is below the optimal level for VDE, and so de-epoxidation rates are retarded and the equilibrium between Z and V starts to shift slightly toward V. In wild-type leaves, lower thylakoidal proton conductivity means that under 1,000 μmol m^{-2} s^{-1} actinic light (i.e. conditions used in Fig. 5), the steady-state *pmf* stays at a much higher level than in *mgd1* (Fig. 6), and so the lumen retains sufficient acidity to maintain high VDE activity.

As yet, we can only speculate about possible reasons why the maximum *pmf* is reduced in *mgd1*. There are no apparent differences in *pmf* between wild-type and mutant plants under low-light intensities (up to 200 μmol m^{-2} s^{-1}; Fig. 6A). This seems to preclude the possibility that the changes in the mutant are due to constitutive increases in the conductivity of the thylakoid membranes caused by alterations in levels of MGDG, because such changes would be expected to alter *pmf* under limiting light intensities as well as at high light intensities. Instead, structural changes of the thylakoids in response to increasing membrane energization may increase the conductivity of the mutant's thylakoid membranes to protons. Interestingly, the increased conductivity becomes apparent under conditions that initiate qE, which is known to involve major structural rearrangements of the PSII-LHCII supercomplexes (Horton et al., 2008). Therefore, MGDG may play an important role during this thylakoid membrane reorganization.

CONCLUSION

The availability of the *mgd1* mutant enabled us to analyze the involvement of MGDG in various processes in vivo. The lack of a measurable effect of the *mgd1* mutation on various chloroplast protein targeting pathways suggested that the residual MGDG in *mgd1* is sufficient to maintain efficient protein transport (Fig. 1). Thus, while the possibility that MGDG is directly involved in chloroplast protein traffic at some level cannot be excluded at this stage, it is possible that the importance of the lipid in these processes has been somewhat overestimated. The low-temperature fluorescence measurements on dark-grown plants revealed the activation of a putative photoprotective mechanism in *mgd1* (Fig. 3, A and B), suggesting that the mutation affects the plant's ability to deal with high light intensities. In accordance with this notion, we confirmed that MGDG deficiency has a negative effect on photosynthetic efficiency at elevated light intensities (Figs. 3C and 4). This is due to a reduction in qN capacity that we ascribe to increased conductivity of the thylakoid membranes, which reduces the maximum *pmf* in *mgd1* by approx-

imately 40%. Consequently, the threshold pH for initiating qE is barely reached, and neither PsbS nor VDE becomes fully activated in the mutant. Impairment of thylakoid membrane energization under high-light conditions may be due to structural rearrangements that occur during the onset of qE. Consideration of our results alongside those obtained using the DGDG-deficient mutant *dgd1* clearly indicates that MGDG and DGDG do not simply provide a membrane environment to physically support the photosynthetic complexes. Rather, these two galactolipids contribute directly to various photosynthesis-related processes with individual contributions that are quite distinct.

MATERIALS AND METHODS

Plant Material and Growth Conditions

Arabidopsis (*Arabidopsis thaliana*) seeds (wild type and *mgd1-1*; both Columbia-0 ecotype) were surface-sterilized, sown on petri plates containing Murashige-Skoog medium, and cold-treated at 4°C (Aronsson and Jarvis, 2002). Thereafter, the seeds were transferred to a growth chamber; after 14 d, seedlings were transplanted to soil. The light regime was 16 h light/8 h dark with a light intensity of approximately 100 to 200 μmol m^{-2} s^{-1}, unless stated otherwise. The *mgd1-1* mutant used throughout this study has been described previously (Jarvis et al., 2000). Together, DNA gel-blot analysis (Supplemental Fig. S2) and genetic, cosegregation analysis (Supplemental Table S1) demonstrated conclusively that there is only a single T-DNA insertion in the mutant and that this insertion is tightly linked to the mutant phenotype.

For the analysis of pigment-protein complexes (Fig. 3), plants were grown on soil either in complete darkness for 5 to 8 d or in the light regime given above for 28 d. Plants used for all other measurements were 35 to 42 d old. Plants used for xanthophyll cycle measurements were kept in darkness for 2 h before applying high-light stress. Light stress was performed for 0, 2, 5, 10, 30, or 60 min at 1,000 to 1,100 μmol m^{-2} s^{-1}.

Chloroplast Isolation and Protein Import

Chloroplasts from 14-d-old plants were isolated according to Aronsson and Jarvis (2002). Template DNA for the Arabidopsis precursors pSS, pL11, and pCF_0II, as well as for atToc33 and atToc34, were amplified by PCR from cDNA clones using M13 primers. Coupled transcription/translation was performed using either a wheat (*Triticum aestivum*) germ extract system or a TNT T7 Quick for PCR DNA system (Promega) containing [^{35}S]Met and T7 RNA polymerase, according to the manufacturer's instructions (Promega). Import reactions were conducted as described (Aronsson and Jarvis, 2002). Briefly, each 150-μL import assay contained 10^7 chloroplasts, 5 mM MgATP, 10 mM Met, and translation mixture not exceeding 10% of the total volume. Import was carried out in white light (100 μmol m^{-2} s^{-1}) at 25°C and was stopped by adding ice-cold HEPES-sorbitol buffer containing 50 mM EDTA. Samples were resolved, fixed, and visualized by fluorography. Quantification employed ImageQuant software (Molecular Dynamics).

For alkaline treatment, import reactions were scaled up three times (3×10^7 plastids) and conducted for 30 min prior to treatment with Na_2CO_3, pH 11.5. Thereafter, envelope membranes were enriched according to Baldwin et al. (2005).

For the thylakoid assays, a 30-min import reaction using 3×10^7 plastids was performed, followed by treatment with thermolysin (final concentration 0.1 mg mL^{-1}) for 30 min at 4°C. Thylakoids were then isolated as described by Rawyler et al. (1992), except that UDP and *p*-hydroxymercuribenzoic acid were omitted from the buffers and MOPS was replaced with HEPES.

Protein Analysis

Concentrations of chloroplast (Fig. 2) and total protein (Fig. 3A, inset; isolated from 5-d-old dark-grown seedlings according to Kovacheva et al. [2005]) samples were determined using the D_C-Protein Assay (Bio-Rad Laboratories). For each sample, an equal amount of protein (10 μg) was separated on SDS-PAGE (Laemmli, 1970) and blotted to nitrocellulose membrane. Membranes were blocked and incubated with primary rabbit antibodies against atToc33, Lhcb2, β-ATPase (all from Arabidopsis), Toc75 (from *Pisum sativum*), D1, PC, VDE (all from *Spinacia oleracea*), PsbB, PsbS, PsaC (all global), PsaD (from *Hordeum vulgare*), and POR (from wheat). A secondary monoclonal anti-rabbit horseradish peroxidase-conjugated immunoglobulin (Amersham Biosciences) was used. Detection was carried out with reagents and the analysis system for ECL (Amersham Biosciences).

Fluorescence Spectroscopy

Fluorescence emission spectra from cotyledons of dark-grown plants or leaves from light-grown plants were measured at 77 K using a Fluorolog-3 spectrofluorometer (Spex Instruments S.A.). The emission was measured as photon emission per unit interval of wavelength. Emission spectra were recorded with an integration time of 0.5 s and the excitation wavelength set to 440 nm, as indicated in the figures. Both excitation and emission monochromators were used with a slit width of 3 nm. The spectra were corrected for the spectral sensitivity of the photomultiplier. Samples were inserted in cylindrical glass cuvettes and stored in liquid nitrogen prior to measurements. Small parts of the hypocotyl accompanied the cotyledons, but the fluorescence from the hypocotyl is negligible compared to the fluorescence from the cotyledons (data not shown). All spectra were smoothed 10 times using a fixed-bandwidth, sharp-cutoff, three-point, low-pass linear digital filter. The spectra shown are averages of five to 10 spectra.

The degree of phototransformation of Pchlide to Chlide in Arabidopsis seedlings was determined after irradiating the samples with three flashes and extracting the pigments into acetone to measure the fluorescence spectra at room temperature. The amount of Chlide found was used to calculate the amount of Pchlide before the flash using a ratio of 1.09 for the fluorescence yield of Pchlide:Chlide. The 1.09 ratio was determined using a PLB preparation (Ryberg and Sundqvist, 1982) measured in darkness, after irradiation and extraction into a 80% (v/v) acetone solution.

Chl Fluorescence Measurements

Chl fluorescence was recorded with a pulse-amplitude modulation fluorometer (Dual-PAM; Heinz Walz). Plants were dark-adapted for 1 h, and fluorescence light response curves were recorded after a 5-min exposure to the photosynthetically active radiation as indicated. PSII quantum yield and linear electron flux were calculated (Genty et al., 1989).

Difference Absorption Spectroscopy

The PSII, cytochrome b_6f complex, and PSI contents were determined in thylakoids, isolated according to Schöttler et al. (2004) as follows. PSI was quantified from measurements of P_{700} difference absorption signals at 830- to 870-nm wavelengths obtained from solubilized thylakoids, according to Schöttler et al. (2007), using a Dual-PAM Chl fluorometer (Heinz Walz). PSII and the cytochrome b_6f complex were determined from difference absorption measurements of cytochromes b_{559} (PSII) and cytochromes *f* and b_6. For these measurements, thylakoids equivalent to 50 μg Chl mL^{-1} were destacked in a low-salt medium to improve the optical properties of the samples (Kirchhoff et al., 2002). All cytochromes were oxidized by application of 1 mM $Na_3Fe(CN)_6$. Subsequent addition of 10 mM sodium ascorbate resulted in the reduction of cytochrome *f* and the high-potential form of cytochrome b_{559}, while cytochrome b_6 and the low-potential form of cytochrome b_{559} were only reduced upon addition of dithionite. At each redox potential, absorption spectra between 540 and 575 nm were determined using a V-550 spectrophotometer with a head-on photomultiplier (Jasco) in which the monochromator slit width was set to 1 nm. The acquired difference absorption spectra were deconvoluted using reference spectra and difference absorption coefficients as described by Kirchhoff et al. (2002). The PSII contents were calculated from the sum of the difference absorption signals arising from the low and high potential forms of cytochrome b_{559}.

The relative stoichiometries of PC per P_{700} were determined using a PC version of the Dual-PAM spectroscope (Dual-PAM-S; Heinz Walz; Schöttler et al., 2007). Measurements were performed on intact leaves prior to thylakoid isolation because some PCs are released from the thylakoid lumen during the isolation, so data obtained on isolated thylakoids are not fully quantitative. The relative PC contents were multiplied by the P_{700} contents determined in thylakoids to obtain estimates of absolute PC contents.

The ECS peak at 517 nm was used as an in vivo measure of the proton motive force across the thylakoid membrane (Kramer et al., 2003; Takizawa

et al., 2007). The difference absorption signal was measured using a KLAS-100 LED-array spectrophotometer (Heinz Walz), allowing the simultaneous measurement of light-induced difference absorption signals at six pairs of wavelengths in the visible range of the spectrum between 500 and 570 nm. The ECS was deconvoluted from signals arising from Z, scattering effects, the C550-signal, and redox changes of the cytochromes, essentially as described by Klughammer et al. (1990), then normalized to the Chl content of the leaf disc. Leaves were illuminated for 10 min prior to each measurement to allow photosynthesis to reach steady state. The maximum amplitude of the ECS was determined after illuminating the leaves with saturating light (2,100 μmol m^{-2} s^{-1}). Saturating illumination was interrupted by short intervals of darkness (15 s), and the dark-interval relaxation kinetics of the ECS and cytochrome *f* reduction were measured. The 15-s dark intervals were sufficient for complete relaxation of the *pmf*. To obtain light saturation curves of the *pmf*, dark-interval relaxation kinetics after illumination at subsaturating light intensities were measured. *Pmf* partitioning into ΔpH and the electrochemical component (ΔΨ) was resolved by analyzing the slowly relaxing phase of the ECS as described by Takizawa et al. (2007).

Photosynthetic Pigment Measurements

Leaf samples were homogenized in liquid nitrogen, and then pigments were extracted at 4°C under low-light conditions using, first, 700 μL of 80% (v/v) acetone, and second, 700 μL of 100% acetone. The two supernatants were combined, and then a 20-μL sample was used immediately for HPLC analysis according to Thayer and Björkman (1990) and Gilmore and Yamamoto (1991), with some alterations. Pigments were separated on a C18 reverse-phase column (Nucleosil 120A C18, 3 μm, 250 × 3 mm, with integrated pre-column; Knauer) using the following solvents: solvent A, acetonitril:methanol: 0.1 M Tris-HCl, pH 8.0 (72:8:3); solvent B, methanol:ethylacetate (68:32). The gradient used was: 0 to 25 min 100% A → 100% B and 25 to 32 min 100% B, followed by 10 min equilibration in 100% solvent A prior to the next measurement, all at a flow rate of 0.4 mL min^{-1}. Detection was carried out at 440 nm, and peaks were identified by comparing their UV spectra and their retention times with commercially available standards.

Sequence data from this article can be found in the GenBank/EMBL data libraries under accession number AAF65066.

Supplemental Data

The following materials are available in the online version of this article.

Supplemental Figure S1. Measurements of VDE activity in wild-type and *mgd1* thylakoids.

Supplemental Figure S2. DNA gel blot indicating that *mgd1* contains a single T-DNA insertion.

Supplemental Table S1. Cosegregation of the *mgd1* phenotype and the T-DNA insertion.

ACKNOWLEDGMENTS

The authors kindly appreciate technical assistance from Monica Appelgren, Markus Nordqvist, Ramesh Patel, Wolfram Thiele, Tony Wardle, and Regina Wendenburg. For antibodies provided, we kindly thank Agrisera AB (Vännäs, Sweden), Hans-Erik Åkerlund (Lund University, Sweden), Adrian Clarke (University of Gothenburg, Sweden), Lars-Gunnar Franzén (Halmstad University, Sweden), Kenneth Keegstra (Michigan State University), and Jürgen Soll (Münich University, Germany). Template DNA was helpfully provided by Dario Leister (Munich University, Germany; pL11) and the Arabidopsis Biological Resource Center (pSS, 188D4T7; pCF_0II, 109L16T7; atToc33, 190I17T7; atToc34; 167B21T7).

Received May 23, 2008; accepted July 14, 2008; published July 18, 2008.

LITERATURE CITED

Aronsson H, Jarvis P (2002) A simple method for isolating import-competent Arabidopsis chloroplasts. FEBS Lett **529:** 215–220

Awai K, Maréchal E, Block MA, Brun D, Masuda T, Shimada H, Takamiya K, Ohta H, Joyard J (2001) Two types of MGD synthase genes, found widely in both 16:3 and 18:3 plants, differentially mediate galactolipid syntheses in photosynthetic and nonphotosynthetic tissues in *Arabidopsis thaliana*. Proc Natl Acad Sci USA **98:** 10960–10965

Baldwin A, Wardle A, Patel R, Dudley P, Ki Park S, Twell D, Inoue K, Jarvis P (2005) A molecular-genetic study of the Arabidopsis Toc75 gene family. Plant Physiol **138:** 715–733

Bédard J, Jarvis P (2005) Recognition and envelope translocation of chloroplast preproteins. J Exp Bot **56:** 2287–2320

Benning C, Ohta H (2005) Three enzyme systems for galactoglycerolipid biosynthesis are coordinately regulated in plants. J Biol Chem **280:** 2397–2400

Block MA, Dorne AJ, Joyard J, Douce R (1983) Preparation and characterization of membrane fractions enriched in outer and inner envelope membranes from spinach chloroplasts. II. Biochemical characterization. J Biol Chem **258:** 13281–13286

Bruce BD (1998) The role of lipids in plastid protein transport. Plant Mol Biol **38:** 223–246

Chen LJ, Li HM (1998) A mutant deficient in the plastid lipid DGD is defective in protein import into chloroplasts. Plant J **16:** 33–39

Chupin V, van't Hof R, de Kruijff B (1994) The transit sequence of a choroplast precursor protein reorients the lipids in monogalactosyl diglyceride cotaining bilayers. FEBS Lett **350:** 104–108

Cruz JA, Avenson TJ, Kanazawa A, Takizawa K, Edwards GE, Kramer DM (2005) Plasticity in light reactions of photosynthesis for energy production and photoprotection. J Exp Bot **56:** 395–406

Douce R, Joyard J (1990) Biochemistry and function of the plastid envelope. Annu Rev Cell Biol **6:** 173–216

Dörmann P, Hoffman-Benning S, Balbo I, Benning C (1995) Isolation of an *Arabidopsis* mutant deficient in the thylakoid lipid digalactosyldiacylglycerol. Plant Cell **7:** 1801–1810

Endo T, Kawamura K, Nakai M (1992) The chloroplast-targeting domain of plastocyanin transit peptide can form a helical structure but does not have a high affinity for lipid bilayers. Eur J Biochem **207:** 671–675

Engdahl S, Aronsson H, Sundqvist C, Timko MP, Dahlin C (2001) Association of the NADPH:protochlorophyllide oxidoreductase (POR) to isolated etioplast inner membranes from wheat. Plant J **27:** 297–304

Erdei N, Barta C, Hideg É, Böddi B (2005) Light-induced wilting and its molecular mechanism in epicotyls of dark-germinated pea (*Pisum sativum* L.) seedlings. Plant Cell Physiol **46:** 185–191

Franck F, Schoefs B, Barthélemy X, Mysliwa-Kurdziel B, Strzalka K, Popovich R (1995) Protection of native chlorophyll(ide) forms and of photosystem II against photodamage during early stages of chloroplast differentiation. Acta Physiol Plant **17:** 123–132

Franck F, Sperling U, Frick G, Pochert B, Cleve B, Apel K, Armstrong GA (2000) Regulation of etioplast pigment-protein complexes, inner membrane architecture protochlorophyllide a chemical heterogeneity by light-dependent NADPH: protochlorophyllide oxidoreductase A and B. Plant Physiol **127:** 1678–1696

Genty B, Briantais JM, Baker NR (1989) The relationship between the quantum yield of photosynthetic electron transport and quenching of chlorophyll fluorescence. Biochim Biophys Acta **990:** 87–92

Gilmore AM, Yamamoto HY (1991) Resolution of lutein and zeaxanthin using a non-endcapped, lightly carbon-loaded C18 high-performance liquid chromatographic column. J Chromatogr **543:** 137–145

Gilmore AM, Yamamoto HY (1993) Linear models relating xanthophylls and lumen acidity to non-photochemical fluorescence quenching. Evidence that antheraxanthin explains zeaxanthin-independent quenching. Photosynth Res **35:** 67–78

Härtel H, Lokstein H, Dörmann P, Grimm B, Benning C (1997) Changes in the composition of the photosynthetic apparatus in the galactolipid-deficient *dgd1* mutant of *Arabidopsis thaliana*. Plant Physiol **115:** 1175–1184

Härtel H, Lokstein H, Dormann P, Trethewey RN, Benning C (1998) Photosynthetic light utilization and xanthophyll cycle activity in the galactolipid deficient *dgd1* mutant of *Arabidopsis thaliana*. Plant Physiol Biochem **36:** 407–417

Hofmann NR, Theg SM (2005) Chloroplast outer membrane protein targeting and insertion. Trends Plant Sci **10:** 450–457

Horton P, Johnson MP, Perez-Bueno MP, Kiss AZ, Ruban AV (2008) Photosynthetic acclimation: Does the dynamic structure and macro-

organization of photosystem II in higher plant grana membranes regulate light harvesting states? FEBS J **275:** 1069–1079

Inoue K, Demel R, de Kruijff B, Keegstra K (2001) The N-terminal portion of the preToc75 transit peptide interacts with membrane lipids and inhibits binding and import of precursor proteins into isolated chloroplasts. Eur J Biochem **268:** 4036–4043

Jarvis P, Dörmann P, Peto CA, Lutes J, Benning C, Chory J (2000) Galactolipid deficiency and abnormal chloroplast development in the Arabidopsis *MGD synthase 1* mutant. Proc Natl Acad Sci USA **97:** 8175–8179

Jarvis P, Robinson C (2004) Mechanisms of protein import and routing in chloroplasts. Curr Biol **14:** R1064–R1077

Jordan P, Fromme P, Witt HT, Klukas O, Saenger W, Krauss N (2001) Three-dimensional structure of cyanobacterial photosystem I at 2.5 Å resolution. Nature **411:** 909–917

Kirchhoff H, Mukherjee U, Galla HJ (2002) Molecular architecture of the thylakoid membrane: lipid diffusion space for plastoquinone. Biochemistry **41:** 4872–4882

Klement H, Helfrich M, Oster U, Schoch S, Rüdiger W (1999) Pigment-free NADPH:protochlorophyllide oxidoreductase from *Avena sativa* L. Eur J Biochem **265:** 862–874

Klughammer C, Kolbowski J, Schreiber U (1990) LED array spectrophotometer for measurement of time resolved difference spectra in the 530-600 nm wavelength region. Photosynth Res **25:** 317–327

Kobayashi K, Kondo M, Fukuda H, Nishimura M, Ohta H (2007) Galactolipid synthesis in chloroplast inner envelope is essential for proper thylakoid biogenesis, photosynthesis, and embryogenesis. Proc Natl Acad Sci USA **104:** 17216–17221

Kovacheva S, Bédard J, Patel R, Dudley P, Twell D, Ríos G, Koncz C, Jarvis P (2005) *In vivo* studies on the roles on Tic110, Tic40 and Hsp93 during chloroplast protein import. Plant J **41:** 412–428

Kramer DM, Cruz JA, Kanazawa A (2003) Balancing the central roles of the thylakoid proton gradient. Trends Plant Sci **8:** 27–32

Kramer DM, Sacksteder CA, Cruz J (1999) How acidic is the lumen? Photosynth Res **60:** 151–163

Krause GH, Weis E (1991) Chlorophyll fluorescence and photosynthesis: the basics. Annu Rev Plant Physiol Plant Mol Biol **42:** 313–349

Krieger A, Weis E (1993) The role of calcium in the pH-dependent control of photosystem II. Photosynth Res **37:** 117–130

Laemmli UK (1970) Cleavage of structural proteins during the assembly of the head of bacteriophage T4. Nature **227:** 680–685

Latowski D, Åkerlund HE, Strzalka K (2004) Violaxanthin de-epoxidase, the xanthophylls cycle enzyme, requires lipid inverted hexagonal structures for its activity. Biochemistry **43:** 4417–4420

Loll B, Kern J, Saenger W, Zouni A, Biesiadka J (2005) Towards complete cofactor arrangement in the 3.0 Å resolution structure of photosystem II. Nature **438:** 1040–1044

Michl D, Robinson C, Shackleton JB, Herrmann RG, Klösgen RB (1994) Targeting of proteins to the thylakoids by bipartite presequences: CFoII is imported by a novel, third pathway. EMBO J **13:** 1310–1317

Miège C, Maréchal E, Shimojima M, Awai K, Block MA, Ohta H, Takamiya K, Douce R, Joyard J (1999) Biochemical and topological properties of type A MGDG synthase, a spinach chloroplast envelope enzyme catalyzing the synthesis of both prokaryotic and eukaryotic MGDG. Eur J Biochem **265:** 990–1001

Pilon M, Wienk H, Sips W, de Swaaf M, Talboom I, van't Hof R, de Korte-Kool G, Demel R, Weisbeek P, de Kruijff B (1995) Functional domains of the ferredoxin transit sequence involved in chloroplast import. J Biol Chem **270:** 3882–3893

Pinnaduwage P, Bruce B (1996) In vitro interaction between a chloroplast transit peptide and chloroplast outer envelope lipids is sequence-specific and lipid class-dependent. J Biol Chem **271:** 32907–32915

Rawyler A, Meylan M, Siegenthaler PA (1992) Galactolipid export from envelope to thylakoid in intact chloroplasts: I. Characterization and involvement in thylakoid lipid asymmetry. Biochim Biophys Acta **1104:** 331–341

Reifarth F, Christen G, Seeliger AG, Dörmann P, Benning C, Renger G (1997) Modification of the water oxidizing complex of the *dgd1* mutant of *Arabidopsis thaliana* deficient in the galactolipid digalactosyldiacylglycerol. Biochemistry **36:** 11769–11776

Runge S, Sperling U, Frick G, Apel K, Armstrong GA (1996) Distinct roles for light-dependent NADPH:protochlorophyllide oxidoreductases (POR) A and B during greening in higher plants. Plant J **9:** 513–523

Ryberg M, Sundqvist C (1982) Characterization of prolamellar bodies and prothylakoids fractionated from wheat etioplasts. Physiol Plant **56:** 125–132

Schleiff E, Soll J, Küchler M, Kühlbrandt W, Harrer R (2003) Characterization of the translocon of the outer envelope of chloroplasts. J Cell Biol **160:** 541–551

Schleiff E, Tien R, Salomon M, Soll J (2001) Lipid composition of outer leaflet of chloroplast outer envelope determines topology of OEP7. Mol Biol Cell **12:** 4090–4102

Schöttler MA, Flügel C, Thiele W, Stegemann S, Bock R (2007) The plastome-encoded PsaJ subunit is required for efficient photosystem I excitation, but not for plastocyanin oxidation in tobacco. Biochem J **403:** 251–260

Schöttler MA, Kirchhoff H, Weis E (2004) The role of plastocyanin in the adjustment of the photosynthetic electron transport to the carbon metabolism. Plant Physiol **136:** 4265–4274

Selstam E, Sandelius AS (1984) A comparison between prolamellar bodies and prothylakoid membranes of etioplasts of dark-grown wheat concerning lipid and polypeptide composition. Plant Physiol **76:** 1036–1040

Selstam E, Schelin J, Brain T, Williams WP (2002) The effects of low pH on the properties of protochlorophyllide oxidoreductase and the organization of prolamellar bodies of maize (*Zea mays*). Eur J Biochem **269:** 2336–2346

Sperling U, van Cleve B, Frick G, Apel K, Armstrong GA (1997) Overexpression of light-dependent PORA or PORB in plants depleted of endogenous POR by far-red light enhances seedling survival in white light and protects against photooxidative damage. Plant J **12:** 649–658

Stroebel D, Choquet Y, Popot JL, Picot D (2003) An atypical haem in the cytochrome b_6f complex. Nature **426:** 413–418

Takahashi Y, Goldschmidt-Clermont M, Soen SY, Franzén LG, Rochaix JD (1991) Directed chloroplast transformation in *Chlamydomonas reinhardtii*: insertional inacxtivation of the *psaC* gene encoding the iron-sulfur protein destabilizes photosystem I. EMBO J **10:** 2033–2040

Takizawa K, Cruz JA, Kanazawa A, Kramer DM (2007) The thylakoid proton motive force in vivo. Quantitative, non-invasive probes, energetics, and regulatory consequences of light induced pmf. Biochim Biophys Acta **1767:** 1233–1244

Thayer SS, Björkman O (1990) Leaf xanthophyll content and composition in sun and shade determined by HPLC. Photosynth Res **23:** 331–343

van't Hof R, Demel RA, Keegstra K, de Kruijff B (1991) Lipid-peptide interactions between fragments of the transit peptide of ribulose-1,5-bisphosphate carboxylase/oxygenase and chloroplast membrane lipids. FEBS Lett **291:** 350–354

van't Hof R, van Klompenburg W, Pilon M, Kozubek A, de Korte-Kool G, Demel RA, Weisbeek PJ, de Kruijff B (1993) The transit sequence mediates the specific interaction of the precursor of ferredoxin with chloroplast envelope membrane. J Biol Chem **268:** 4037–4042

Webb M, Green B (1991) Biochemical and biophysical properties of thylakoid acyl lipids. Biochim Biophys Acta **1060:** 133–158

Yamamoto HY (2006) Functional roles of the major chloroplast lipids in the violaxanthin cycle. Planta **224:** 719–724